UNIVERSITY
OF
JOHANNESBURG

PROGRAM	:	**MECHANICAL ENGINEERING**
SUBJECT	:	**SCIENCE OF MATERIAL 3A**
CODE	:	**MTK3A11**
DATE	:	8 JUNE 2019 (WINTER EXAMINATION)
DURATION	:	3 HOURS (1-PAPER)
TOTAL MARKS	:	100

EXAMINER	:	Mr. T Mathonsi
MODERATOR	:	Prof. RF Laubscher
NUMBER OF PAGES	:	6 PAGES

INSTRUCTIONS	:	QUESTION PAPERS MUST BE HANDED IN.
REQUIREMENTS	:	ANSWER BOOKLET.

INSTRUCTIONS TO CANDIDATES:

PLEASE ANSWER ALL QUESTIONS

QUESTION 1 [12]

Discuss the difference in composition, heat treatments/cooling rates, and microstructure of gray, white, and malleable cast iron. (12)

Hint: Schematically illustrate and name the microstructures resulting from fast, moderate and slow cooling rates during the production of these cast irons.

QUESTION 2 [68]

Read the following case study of a failure analysis that was performed on a stainless steel reducer and answer the questions that follow:

A 200 x 150 mm, 316L stainless steel reducer was sent for failure analysis, shown in Figure 2.1. It had been in service for 13 months when a leak was noticed. The reducer was installed on an acid storage tank. The anodically protected carbon steel tank, contained concentrated 93% sulphuric acid. The flow rate through the reducer was 1500L/min.


Figure 2.1—316L reducer.

The tank was originally designed with a 100 mm diameter carbon steel nozzle, at floor level, that connected directly to a valve shown in Figure 2.2(a). This lasted seven to eight years without incident. The design was changed to accommodate renovations so that a 200 mm carbon steel nozzle was installed 150 mm above the tank floor. This nozzle leads into the failed reducer, which then connects to a valve composed of alloy steel, as illustrated in Figure 2.2 (b). The valve then leads to a 150 mm pipe made of 316L stainless steel in which no problems were found.
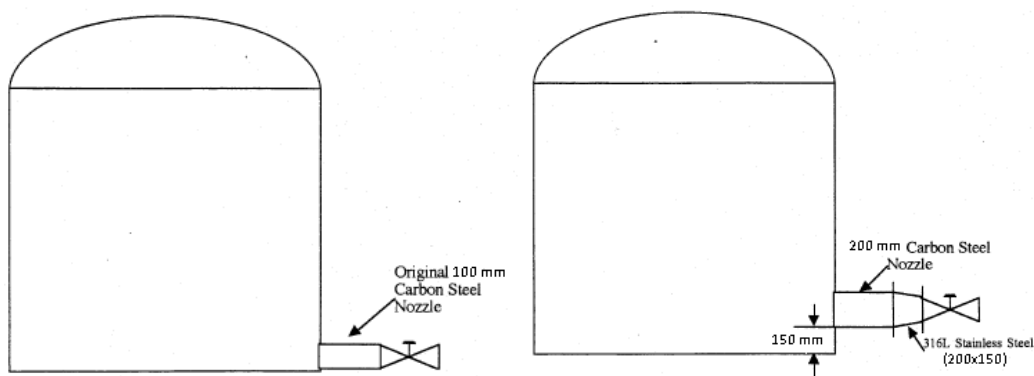
Figure 2.2 (a) Old tank installation. (b) Tank installation at the time of reducer failure.

Observations: *Visual examination of the reducer revealed an area at the top where little to no damage was observed (Figure 2.3). This area, which was probably an air pocket, extended from the top of the 200 mm diameter flange into the reducing pipe where it stopped just before the 150 mm diameter flange. Damage in this area consisted of minor pitting shown in Figure 2.4. Damage, resembling a honeycomb structure in places, was most severe just below the air pocket in the reducing pipe near the 150 mm diameter end (Figure 2.5 (a) and (b)). The arrow in Figure 2.5 (a) indicates where the leak occurred. The leak was discovered on the outside of the reducer (Figure 2.6). The damage becomes less severe in the pipe section towards the bottom. Only pitting was found in both the 200 and 150 mm flanges.*
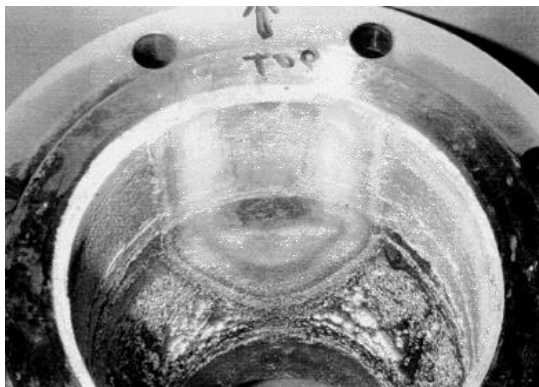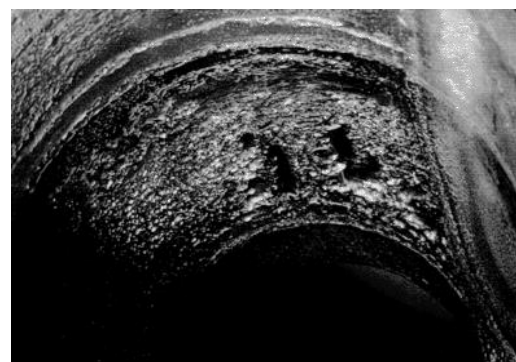

Figure 2.3—Photograph of the top insider of the reducer showing the area at the top where little damage occurred.

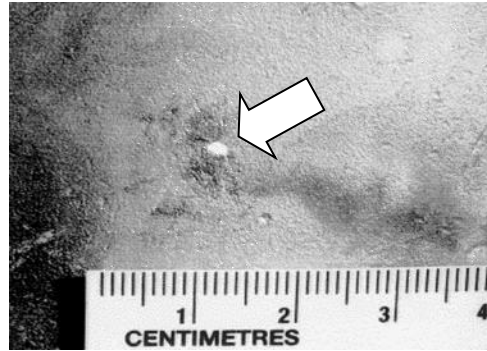*Figure 2.4—Microphotograph of pitting in air pocket. 15X*


(a)

(b)

Figure 2.5—Photographs showing areas to the (a) right and (b) left of the top relatively undamaged surface. The arrow in (a) indicated where the leak occurred.

Figure 2.6—Photograph taken on the outside of the reducer showing the hole where the reducer leaked.

Closer examination of the inside surface of the reducer with a SEM revealed dimples (Figure 2.7). These features are typical of ductile deformation. The orientation of the features also follows the direction of liquid flow, which indicates erosion of the surface. Pitting and uniform corrosion was also found in this region (Figure 2.8).
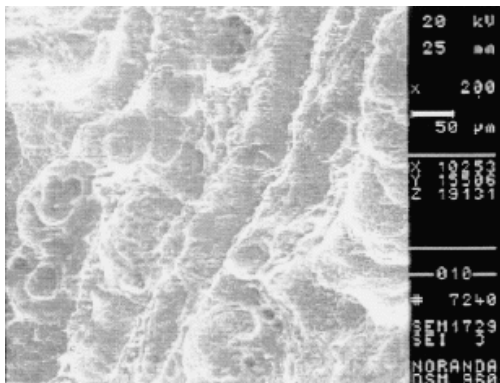
Figure 2.7—SEM photograph of the inside surface of the reducer in the damaged area. 200X
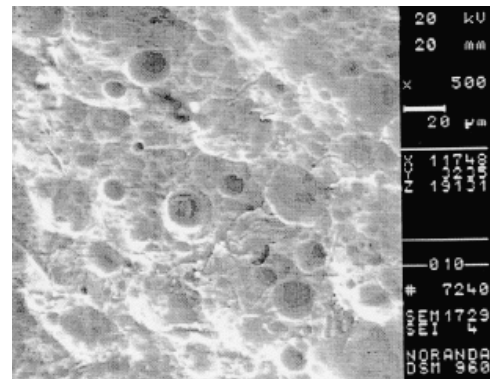
Figure 2.8—SEM photograph of the inside surface of the reducer in the damaged area. 500X

Chemical analysis of the flange and the pipe revealed that they both conform to AISI-SAE standards for 316L stainless steel (Table 2.1)

Table 2.1—Result of chemical analysis.

Element	Analysed Composition of Flange (%)	Analysed Composition of Pipe (%)	AISI-SAE 316L Standard Composition Ranges (%)
Carbon	0.031	0.034	0.03 max.
Manganese	1.85	1.28	2.00 max.
Silicon	0.57	0.35	1.00 max.
Phosphorus	0.014	0.011	0.045 max.
Sulphur	0.023	0.001	0.03 max.
Chromium	16.53	17.47	16.0-18.0
Nickel	10.85	11.46	10.0-14.0
Molybdenum	2.16	2.08	2.0-3.0

Conclusions and Recommendations: *A combination of two mechanisms caused the failure. Severe turbulence in the reducer caused a degradation of the passive layer that protects the stainless steel from corrosion. This would have left the system open to pitting and uniform attack, which in turn would*

have led to failure. The top of the reducer was probably protected by the presence of an air pocket. The second mechanism was cavitation erosion.

2.1. Stainless steels are categorised according to microstructure. List 4 types of stainless steels, their general application (according to their general properties), hardenability characteristics, and an example of each type. (16)

2.2. Use appropriate phase diagrams to illustrate and explain why ferritic and austenitic stainless steels are not heat treatable. (10)

2.3. Pitting and uniform corrosion was observed in the reducer. Define these types of corrosion and comment on the mechanisms responsible for causing these types of corrosion. (4)

2.4. Many factors can control the tendency for a material to corrode. Discuss the effect of material properties and the environment when considering corrosion.
(12)

2.5. The carbon steel tank was anodically protected. Explain the difference between anodic protection, cathodic protection, and galvanic protection. (6)

2.6. List 2 major effects of the following alloying elements found during chemical analysis of the flange and the pipe:

2.6.1. Manganese
2.6.2. Sulphur
2.6.3. Chromium
2.6.4. Nickel (8)

2.7. Was a suitable material selected and used for the reducer? Motivate. (4)

2.8. Define cavitation erosion. (4)

2.9. What preventative measures can be taken to avoid future failures of this nature.
(4)

QUESTION 3 **[20]**

3.1 Define the following failure mechanisms

3.1.1 Ductile fracture

3.1.2 Fatigue

3.1.3 Creep

<div style="text-align:right">(6)</div>

3.2 A structural component in the form of a wide plate, shown below is to be fabricated from 4340 steel. Two sheets of this alloy, each having a different heat treatment are available. Material A has a yield strength of 860 MPa and a plane strain fracture toughness of 98.9 MPa$\sqrt{m}$. Material B a yield strength of 1515 MPa and a plane strain fracture toughness of 60.6 MPa$\sqrt{m}$.

3.2.1 For each alloy, determine whether or not plane strain conditions prevail if the plate is 10 mm thick, given: (4)
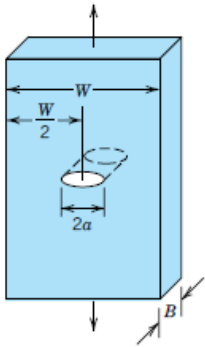
$$K_{Ic} = Y\sigma\sqrt{\pi a} \text{ if}$$

$$B \geq 2.5\left(\frac{K_{Ic}}{\sigma_y}\right)^2$$

3.2.2 It is possible to detect flaw sizes bigger than 3 mm using NDT methods. Determine whether the critical flaw size is subject to detection if plane strain conditions prevail and the design stress level is one-half of the yield stress and Y=1.0. (5)

3.4 Explain martempering by illustrating the heat treatment process on a TTT diagram and referencing the obtained microstructure and expected mechanical properties. (5)